IJCTA, 9(24), 2016, pp. 331-342 ISSN: 0974-5572

Minimization of The DC Component in Transformerless Photovoltaic Inverter System by Fuzzy Controller

G. Venkatesh*, B. Murali Mohan and M. Neha Sarath Chandrika*****

ABSTRACT

In the power systems the dc component can affect the operating point of the transformers. The transformer cores are determined into unidirectional saturation with consequent larger excitation current. The transformer reduces the inrush currents and maintains required voltages but for low frequency (50 or 60 HZ) transformer is bulky, heavy, and expensive so its power loss brings down the overall system efficiency. Then the PV array is connected to the grid via a two level inverterthree phase voltage source and an LCL filter is replaced instead of the transformer. The edge for dc module in the grid side ac currents is below 0.5% of the rated current. The dc component can cause dc-link voltage ripple,line frequency power ripple and further second order harmonic in anac current. The dc component injected to the grid can disturb the normal operation of the loads connected to the grid and causes torque ripple, extra loss in ac motors. To reduce the dc component in three phase ac currents the real solution is shown in this paper is to mimic the blocking capacitors used for the dc component reductionis called as virtual capacitor. The "virtual capacitor" is attained by adding an integral of the dc module in the current response path. The accurate extraction of the dc componentcan achieve the control, harmonic conditions and approved effective even under grid frequency variation. A proportional integral resonant controller is additional designed to regulate the dc and line frequency module in the current loop to deliveraccurate control of the dc current.Here fuzzy logic is used for controlling compared to other controllers. The Simpered Systems tool has demonstrated that the joint system will at the same time inject maximum power from a PV unit and compensate the harmonic current drained by nonlinear loads.

***Key words*:**Controller, dc component, proportional integral resonant (PIR),transformer less three-phase PV inverters, virtual capacitor.

1. INTRODUCTION

Grid associated photovoltaic (PV) systems often include a line transformer between the grid and power converter. The transformer promises galvanic isolation between the grid and the PV systems. Further, it ensures that no direct current (dc) is injected to the grid. However, the low frequency (50 or 60 Hz) transformer is large, heavy and expensive its power loss brings down the overall system efficiency.

The dc component can have negative impacts on the power system in the following ways:

1) In the power system the dc component can affect the operating point of the transformers. With consequent larger excitation current the transformer cores are driven into unidirectional saturation. The service lifetime of the transformer is reduced as a result with additional increased hysteresis, eddy current losses and noise.
2) The dc component can circulate between inverter phase legs and inverters in a paralleled arrangement. The dc component circulation affects the loss distribution and even current among paralleled inverters.
3) The corrosion of grounding wire in substations is intensified.

* Assistant Professor, Dept. of EEE A.I.T.S-Rajampet, A.P, INDIA, *Email: gchinna255@gmail.com*

** Assistant Professor, Dept. Of EEEPG Student, Dept. of EEE, *Email: aitseee.bmm@gmail.com*

*** P.G. Student, A.I.T.S-Rajampet, A.P, INDIA A.I.T.S-Rajampet, A.P, INDIA, *Email: nehasarathchandrika@gmail.com*

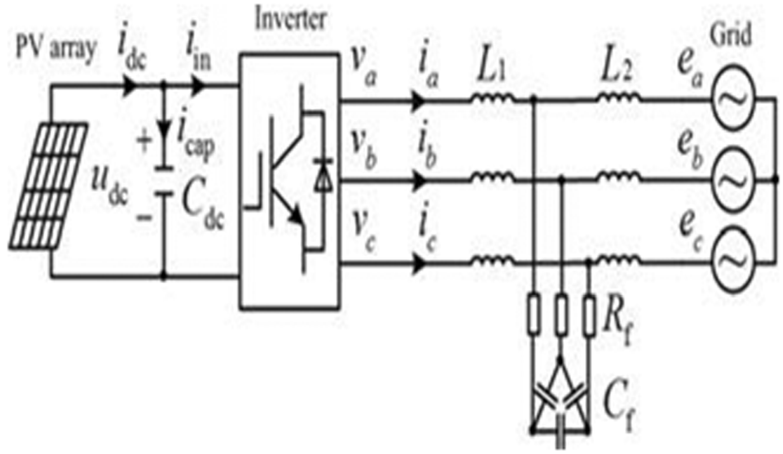

Figure 1: Transformer less three phase PV inverter system.

In the proposed control plan, an exact dc component quantity and extraction is critical.Here several devices can be used to amount the dc module, e.g., by shunt resistors, voltage transformers, mutual coupled inductors, and integral methods, etc. Among them, only the integral methods do not need additional hardware.

So a new integral method based on the sliding window double time and iteration algorithm integral is presented. This technique is active in the extraction of the dc module even for currents with frequency fluctuations and harmonics.

2. IMPACT OF THE DC COMPONENTS ON PV SYSTEMS

A typical three phase transformer less PV inverter system is shown in Fig. 1. The PV array is connected to the grid via three phase voltage source two level inverter and an LCL filter. The capacitors of the LCL filter are configured with a delta or star connection. In this paper, to reduce the required capacitor and cost a delta connection is used as *opposed to the star connection, which has the benefit* of smaller short-circuit current. The dual closed loop control strategy comprises a current and a dc-link voltage loop in the synchronous rotational frame, is a common control strategy in three phase PV inverters.

$$\begin{cases} Fa = Fa0 + Fa1 \\ Fb = Fb0 + Fb1 \\ Fc = Fc0 + Fc1 \end{cases}, \quad \begin{cases} F\alpha = F\alpha 0 + F\alpha 1 \\ F\beta = F\beta 0 + F\beta 1 \end{cases}, \quad \begin{cases} Fd = Fd0 + Fd1 \\ Fq = Fq0 + Fq1 \end{cases} \tag{1}$$

Where the subscript 0 denotes the dc component and the subscript 1 denotes the line-frequency component. If there are dc components in the abc coordinate, they will also exist in the form of dc or line-frequency components in αβ and dq coordinates, respectively. In a three-phase three-wire system, there is no current flowing through the neutral point and hence the line frequency is

$$\begin{cases} Fa0 = Fb0 + Fc0 = 0 \\ Fa1 = Fb1 + Fc1 = 0. \end{cases} \tag{2}$$

With (1) and (2), the coordinate transformations of the dc components from abc coordinate to αβ and dq coordinate can be expressed as

$$\begin{pmatrix} F\alpha 0 \\ F\beta 0 \end{pmatrix} = \frac{2}{3} \begin{pmatrix} 1 - \frac{1}{2} - \frac{1}{2} \\ 0 \frac{\sqrt{3}}{2} - \sqrt{3/2} \end{pmatrix} \cdot \begin{pmatrix} Fa0 \\ Fb0 \\ Fc0 \end{pmatrix} = \begin{pmatrix} Fa0 \\ \frac{\sqrt{3}}{3Fb0} - \sqrt{3}/3Fco \end{pmatrix} \tag{3}$$

$$\begin{pmatrix} Fd1 \\ Fq1 \end{pmatrix} = \frac{2}{3}\begin{pmatrix} \cos\theta \sin\theta \\ -\sin\theta \cos\theta \end{pmatrix} \cdot \begin{pmatrix} 1 - \frac{1}{2} - \frac{1}{2} \\ 0 \frac{\sqrt{3}}{2} - \frac{\sqrt{3}}{2} \end{pmatrix} *$$

$$\begin{pmatrix} Fa0 \\ Fb0 \\ Fc0 \end{pmatrix} = \begin{pmatrix} Fa0\cos\theta + \frac{\sqrt{3}}{3}\left[Fa0 - Fco\right]\sin\theta \\ \frac{\sqrt{3}}{3}\left[Fb0 - Fco\right]\cos\theta - Fa0\sin\theta \end{pmatrix} \tag{4}$$

Where θ is the angle between the dq coordinate and abc coordinate for example, the grid angle in a grid voltage oriented vector control.

Asin (3) and (4) the coordinate transformation, F_{a0}, $F_{b0}$and F_{c0} (dc components) in the stationary abc frame can be transformed into $F_{\alpha 0}$ and $F_{\beta 0}$ in the stationary αβ frame and then F_{d1} and F_{q1} (line frequency) in dq frame.

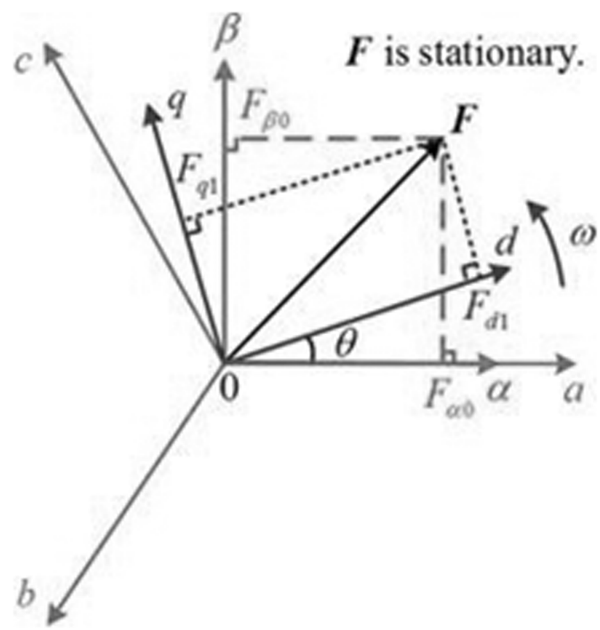

Figure 2: Coordinatetransformation of dc components.

$$P_{ac} = 3/2\begin{bmatrix} Ud \\ Uq \end{bmatrix} T.\begin{bmatrix} Id \\ Iq \end{bmatrix} = 3/2\begin{bmatrix} ud0 + ud1 \\ uq0 + uq1 \end{bmatrix} T.\begin{bmatrix} id0 + id1 \\ iq0 + iq1 \end{bmatrix}$$

$$= \frac{3}{2}\begin{bmatrix} ud0id0 + q0iq0 + \\ DC\ component \\ +ud0id1 + ud1id0 + uq0iq1 + uq1iq0 + \\ Line - frequency\ fluctuation \\ ud1id1 + uq1i1 \\ 2nd\ fluctuation \end{bmatrix} \tag{5}$$

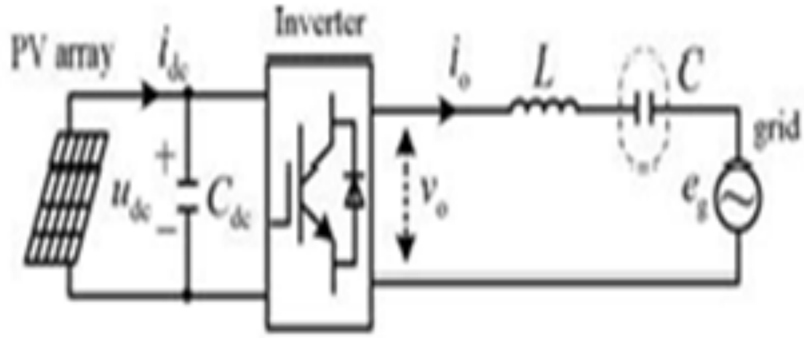

(a) Circuit diagram of a single-phase grid-connected PV inverter with the blocking capacitor

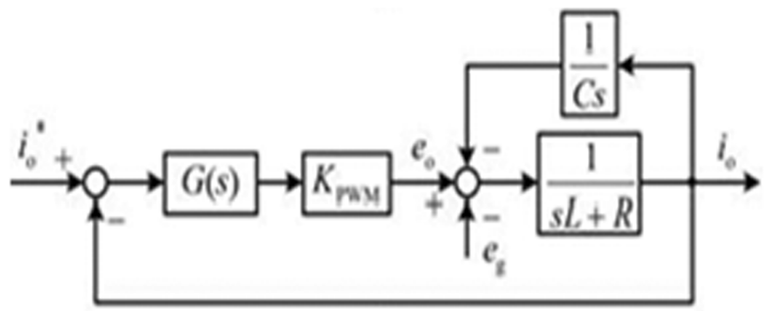

(b) Current control loop diagram,

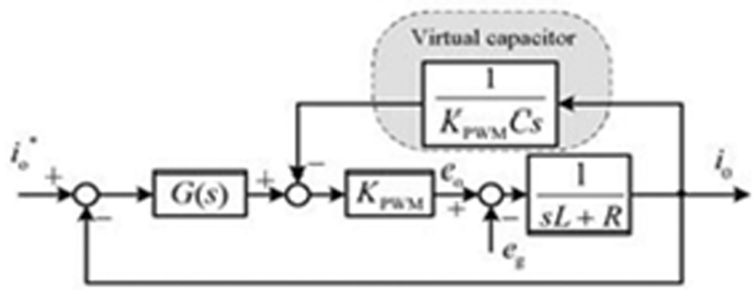

(c) Equivalent transformation of the current control loop with virtual capacitor concept.
Figure 3: Virtual capacitor concept of a single-phase grid-connected PV inverter

$$q_{ac} = 3/2\left\|\begin{bmatrix} Ud \\ Uq \end{bmatrix} T * \begin{bmatrix} Id \\ Iq \end{bmatrix}\right\| = 3/2\left\|\begin{bmatrix} ud0 + ud1 \\ uq0 + uq1 \end{bmatrix} T * \begin{bmatrix} id0 + id1 \\ iq0 + iq1 \end{bmatrix}\right\| \text{ (T = transpose)}$$

$$= \frac{3}{2}\begin{bmatrix} ud0id0 + q0iq0 + \\ DC\ COMPONENT \\ +ud0id1 + ud1id0 + uq0iq1 + uq1iq0 + \\ LINE - FREQUENCY\ FLUCTUATION \\ ud1id1 + uq1iq1 \\ 2nd\ FLUCTUATION \end{bmatrix} \tag{6}$$

As shown, both the active and reactive power contains a line frequency, aconstant dc power and a second order power fluctuation due to the dc component in the current and voltage undesired. Further, with grid voltage orientated vector control under unity power factor operation for PV applications, where u_{q0} = 0, i_{q0} = 0, (5) and (6) can be simplified as (7) and (8) if assuming the second order fluctuations is negligible compared to the other two components.

$$p_{ac} = \frac{3}{2}\begin{pmatrix} ud0id0 \\ DC\ component \\ +ud0id1 + ud1id0 \\ Line - frequency\ fluctuation \end{pmatrix} \tag{7}$$

$$q_{ac} = \begin{pmatrix} uq1id0 - ud0iq1 \\ Line - frequency\ fluctuation \end{pmatrix} \tag{8}$$

3. MINIMIZATION OF DC COMPONENT IN THREE-PHASE GRID-CONNECTED PV SYSTEMS

3.1. Virtual Capacitor Concept of Single-Phase Grid-Connected PV Inverters

To block the dc component put a capacitor *C* in series with the ac side of the inverter shown in Fig. 4(a). However, in order to reduce the capacitive reactance at other frequencies, the value of the capacitor must be large; it increases the size and cost of the system. This series capacitor may also disturb the system dynamic response and reduce transmission efficiency. However, the physical capacitor is replaced by software based method and advanced control strategy mimics the operation of the series capacitor in a single phase PV system.

$$\text{L (di0/dt)} + 1/\text{C}\int i0dt + Ri0 = eg - v0 \tag{9}$$

$$I_0(s) = \frac{Cs}{LCs2 + RCs + 1}\left[E_g(s) - V_0(s)\right] \tag{10}$$

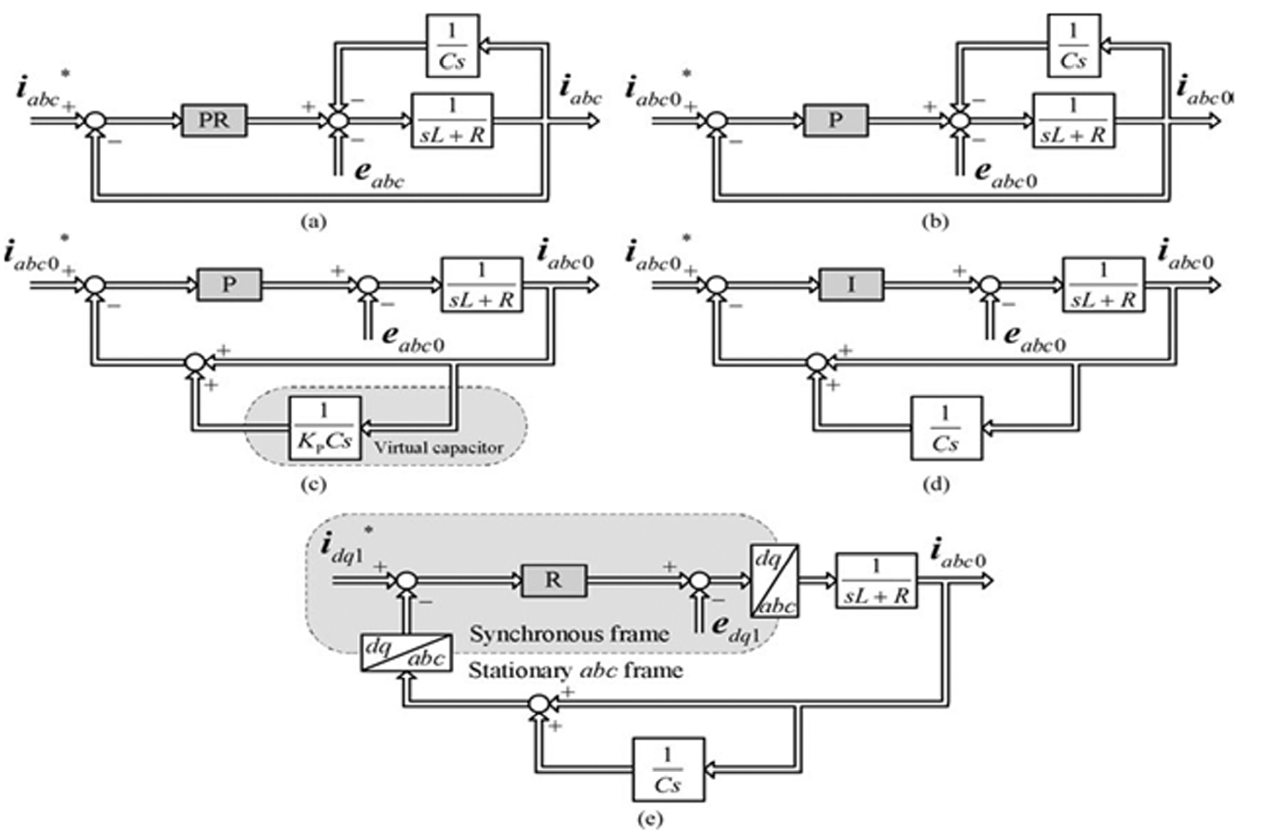

Figure 4: Virtual capacitor implementation for a three-phase PV inverter: (a) current control loop in stationary a-b-c frame, (b) dc component control loop in stationary a-b-c frame, (c) equivalent transformation of the dc component control loop with virtual capacitor, (d) dc component control loop based on an integral (I) controller, and (e) dc component control loop in a mixed frame (d-q and a-b-c).

Where v_o and i_o are the inverter output voltage and current,e_g is the gird voltage; $V_o(s)$, $I_o(s)$ and $E_g(s)$ are the Laplace transforms of v_o, $i_o$and e_g in the frequency domain, L is the filter inductance; R is the line equivalent resistance and C is the blocking capacitor.

Substituting the operators in (10) with jω, I_0 (jω) equals zero when ω = 0(dc). This indicates that the blocking capacitor can minimize the dc componenteffectively.

3.2. Mathematical Model of the Three-Phase PV Inverter with Blocking Capacitors in the Synchronous Frame

Based on the virtual capacitor concept in the single phase system aims to derive the three phase system models with blocking capacitors in different frame and inspect the correctness of applying the virtual capacitor concept to three-phase systems in each frame. Fig. 5 shows the circuit diagram of a three-phase PV inverter with blocking capacitors (C).

$$\begin{aligned} Ldi_a/dt + 1/C\int = e_a\text{-}v_a \\ Ldi_b/dt + 1/C\int = e_b\text{-}v_b \\ Ldi_c/dt + 1/C\int = e_c\text{-}v_c \end{aligned} \tag{11}$$

Where L is the equivalent inductance which includes Inverterside inductance L_1 and the grid sideinductance L_2.The definitions of other variables in (11) are denoted in fig (5). Especiallyv_a, v_b and v_c are the average values of inverter side voltage over a switching period. Note that the inverter duty cycle I not included in the average model in (11) to simplify the control design. A more rigorous invertor small signal model can be founding.

$$\begin{cases} \dfrac{Ldi\alpha}{dt} + 1/C\int i\alpha dt + Ria = e\alpha - v\alpha \\ \dfrac{Ldi\beta}{dt} + \dfrac{1}{c}\int i\beta dt + Ri\beta = e\beta - v\beta \end{cases} \tag{12}$$

In order to further derive the models in frequency domain on the synchronous rotational dq frame, complex vectors are synthesized from scalars in ±² and dq frame as shown

$$\begin{cases} f\alpha\beta = f\alpha + jf\beta \\ fdq = fd + jfq \end{cases} \tag{13}$$

Where f is general complex vector which can representsvoltage and current. With the complex vector expression in (13), the system model in α-β.

Frame in (12) can be transformed to the complex vector form as given in

$$\text{L(di}\alpha\beta\text{/dt+1}\int i\alpha\beta dt + Ri\beta = e\alpha\beta - v\alpha\beta \tag{14}$$

$$I_{\alpha\beta}(s) = \frac{Cs}{LCs2 + RCs + 1}\ [E_{\alpha\beta}\ (s)\text{-}V_{\alpha\beta}(s)] \tag{15}$$

$$\text{Idq(s)} = \frac{C[s + jw]}{Ls[s + jw]2 + RC[s + jw] + 1} *[\text{Edq(s)-Vdq(s)}] \tag{16}$$

Substituting (13) in (16), the mathematical model for the three phase system with blocking capacitors in dq frame can be derived as

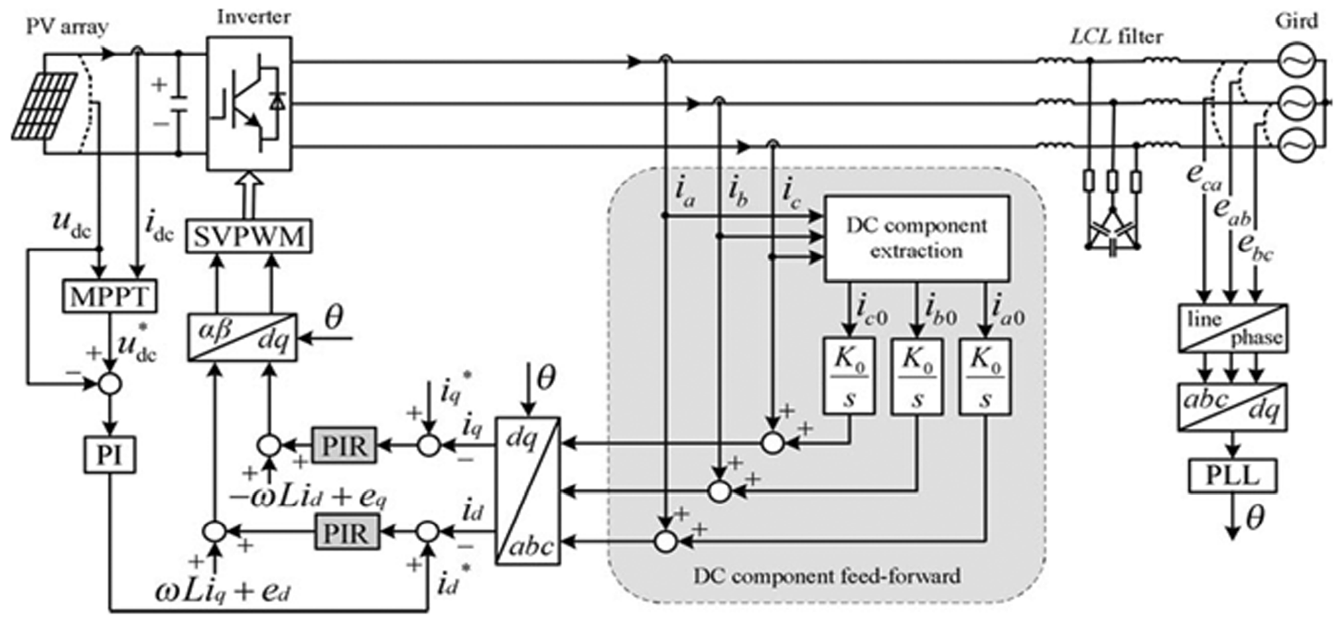

Figure 5: DC component minimization strategy based on dc component feed-forward and PIR controllers.

$$\{Id(s)\ LCs\ 2 + RCs - Lw2 + 1] - Iq(s)\ [2LSws + RCw\} =$$
$$[Ed\ (s) - Vd(s)]\ Cs - [Eq(s) - Vq(s)]$$
$$Cw.Id(s)\ [2LCws + RCw] + Fq(s)\ [LCs2 + RCs - LCw2 + 1] =$$
$$Ed(s) - Vd(s)]Cw + Eq(s) - Vq(s)]\ Cs \tag{17}$$

Shown in (17), after adding blocking capacitors to the ac side of the power circuit, there are strong couplings between the d and q axis is very difficult to be decoupled. This specifies that the virtual capacitor should not be in the standard synchronous rotational dq frame but in the stationary abc frame.

3.3. DC Component Minimization in Three-Phase PV Inverters with DC-Component Feed-Forward and PIR Controllers

Based on the above analysis, this section investigates how to implement the "virtual capacitor" concept for three phase systems in the stationary frame and to be further integrated to the standard PV inverter current control loop in the dq frame with a PIR controller. The standard three phase inverterloop normally adopts a proportional integral (PI) controller to regulate the d-axis and q-axis currents. The PI controller in dq frame is equivalent to a proportional-resonant (PR) controller in the stationary abc frame given the resonant frequency of the R controller andselected as the line rotational frequency. Therefore, the current control loop of three phase inverters with blocking capacitors in stationary abc frame can be represented as shown in Fig. 6(a), where the variables of subscript abcdenote the vectors of the three phase voltages and currents. The gain of the pulse width modulator (KPWM) is assumed to be unity to simplify the derivation.

4. DC COMPONENT EXTRACTION BASED ON SLIDING WINDOW ITERATION

In the control strategy shown in Fig. 7, an accurate dc component measurement and extraction is the key to implement the virtual capacitor concept and achieve the overall dc component minimization.

As mentioned, the dc component needs to be reduced within 0.5% of the rated output current. Compared with the ac component, the dc component is very small and an accurate dc component extraction is stimulating. In PV inverters, the Hall Effect current sensors are widely used to measure the ac side currents (including both ac and dc components) due tothesmallersize, isolated output, and wide bandwidth (e.g., from dc to several hundred kilohertz). An integral method based on the sliding window iteration algorithm is used in this paper to extract the dc component from the ac side currents.

Taking the ac side Phase A current i_a can be expressed in (18) if considering both the dc component and other ac components of different frequencies (e.g., harmonics).

$$ia = ia0 = \sum_{h=1,2,3}^{n} \sin\left[2\pi f1t + \psi h\right] \tag{18}$$

Where i_{a0} is the dc component, f_1 is the line frequency. I_h, hf_1, and $\tilde{O}_h$ are the amplitude, frequency, and phase angle of the fundamental and harmonic components. Averaging the integration of (18) in the interval from t_0 to $t_0 + T$ yields

$$\frac{1}{T}\int_{t0}^{t0+T} iodt = 1/T\left[\int_{t0}^{t0+T} ia0dt + \int_{t0}^{t0+T} \sum_{h=1,2,3...} In\sin\left[2\pi f1t + \varphi hdt\right]\right] \tag{19}$$

When $T = T_1 = 1/f_1$, the second term in the right side of (19) becomes

$$\int_{t0}^{t0+T} \sum_{h=1,2,3......} Ih\sin\left[2\pi f1t + \varphi h\right]dt = 0 \tag{20}$$

Hence the (19) and (20) of dc component i_{a0} can be obtained by

$$ia0 = \frac{1}{T1}\int_{t0}^{t0+T} iadt \tag{21}$$

The next step is to implement the expression in (21) toobtain the dc component ia0 accurately without significant calculation burden. If assuming the number of sampling times in a fundamental period (T_1) is N, dt in (21) can be substituted by the sampling interval Δt and $\Delta t = T_1/N$. If τ is defined as t/N, then Ia (kτ) is the kth sampling value. Substituting the definiteintegration in (21) by the accumulation of the integrand, the discrete expression of ia0 is given by

$$ia0 = \frac{1}{N\Delta T}\sum_{k=0} ia\left(KT\right)\Delta t = \frac{1}{N}\sum_{k=0}^{N-1} ia\left(KT\right) \tag{22}$$

To achieve a real time dc component extraction the sampling values for N_1timesinonefundamental period is therefore significant given a high sampling frequency. To decrease the amount of calculation, sliding window iteration is used in (23) to replace (22)

$$ia0 = \frac{1}{N}\sum_{k=Ncut-N+1}^{Ncut} i0\left(KT\right) = \frac{1}{N}\sum_{k=Ncut-N}^{Ncut-1} ia\left(KT\right) - ia\left(Ncut - NT\right) + ia\left(NcutT\right) \tag{23}$$

Where N_{cur} is sliding pointer represent the current sampling point. After completing the summation of one fundamental period for initialization, N–1 additions of (22) is simplified as one addition and one subtraction of (23). As a result, the amount is reduced. The dc component calculation method based on the sliding window iteration is illustrated in Fig. 8.

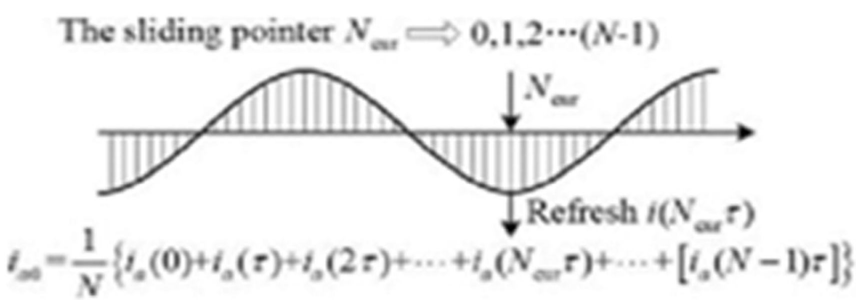

Figure 6: Diagram of the dc component calculation based on the sliding window iteration.

Which contains a dc component (step signal at 0.08 s),f1 = 49 .5Hz, fifth and seventh order harmonics

$$ia = 0\ .5\varepsilon(t - 0.08) + 10 \sin(2\pi f1t) + 1.5 \sin(10\pi f1t) + 0.5 \sin(14\pi f1t) \quad (24)$$

The dc component extraction method is implemented and tested in MATLAB/Simulink. Herethefuzzy controller is used compared to alternative controllers because of its accurate performance. Simulation results of the dc component extraction method under frequency deviation and with harmonics are shown in Fig. 9. Fig. 9(a) shows the measured ac side current signal which contains fifth and seventh harmonics as well as a dc component appearing from 0.08 s. Fig. 9(b) shows the dc component in the current signalwithamplitudeof0.5A. Fig.9(c)shows the simulation results of the dc component extraction method. As seen, although the average value of the dc component is estimated correctly as 0.5A, line frequency fluctuation exists in i_{a0} because of the frequency deviation.

5. PIR CONTROLLER DESIGN

As mentioned, when taking the dc component in the ac-side currents into account, the current loop in the dq frame is composed of both a dc component and a line-frequency component (negative sequence). The dc component in the rotational frame comes from the line-frequency ac components in the phase currents.

From the dc component the phase currents provide an effective control for both dc and line frequency signals in the dq frame and a proportional integral resonant (PIR) controller is used. Taking the d-axis

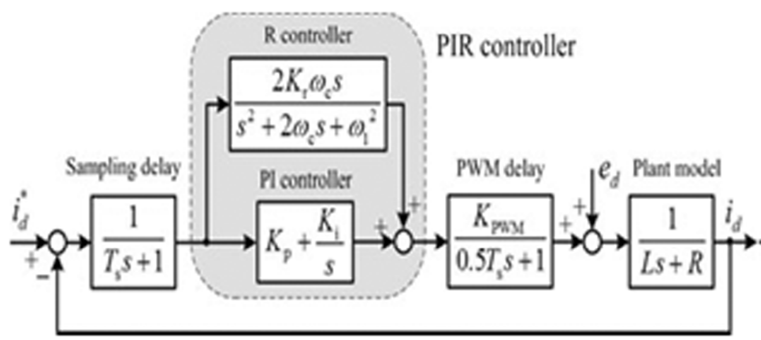

Figure 7: d-axis current control loop based on the PIR controller.

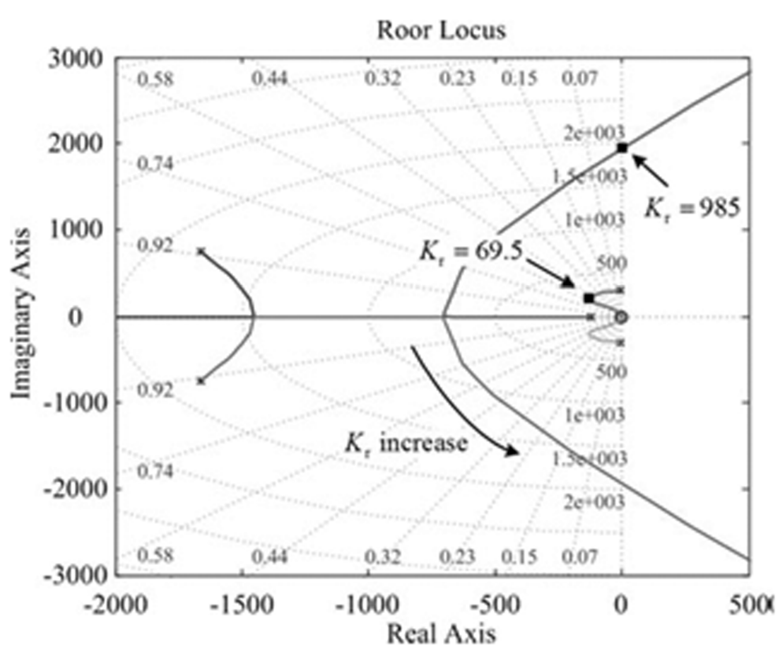

Figure 8: Root locus of the current loop with Kr varying from 0 to infinite.

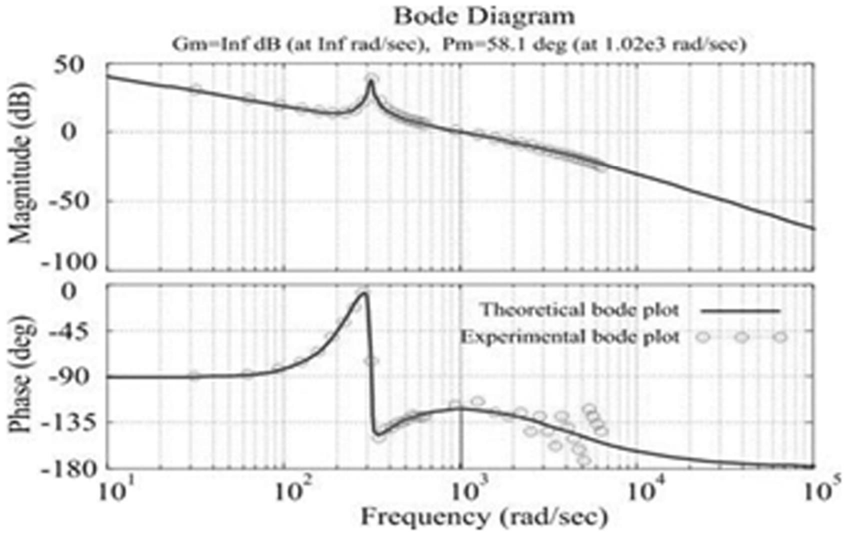

Figure 9:Theoretical open-loop bode plot of the current loop with a PIR controller for L =2 .7mH, R = 0 .3Ω,ω_c = 5rad /s, K_p = 2 .7, Ki = 300, and Kr = 69 .5.

current control loop the sampling delay and the PWM delay, the current control loop based on the PIR controller is shown in Fig. 10.

As expected, the bode plot has both high gain at dc and line frequency. The phase margins (Pm = 58.1°) indicates that the designed current loop is stable.

The system is simulated in MATLAB/Simpered Systems and Fuzzy simulated system is shown in fig.10 to the accurate extraction of the dc component can achieve the control, harmonic conditions and approved effective even under grid frequency variation.

6. FUZZY LOGIC CONTROL

The Fuzzy logic control consists of set of linguistic variables. Here the PI controller is replaced with Fuzzy Logic Control. The mathematical modeling is not required in FLC. FLC consists of

6.1. Fuzzification

Membership function values are assigned to linguistic variables. In this scaling factor is between 1 and -1.

6.2. Inference Method

There are several composition methods such as Max-Min and Max-Dot have been proposed and Min method is used.

6.3. Defuzzificaion

A plant requires non fuzzy values to control, so defuzzification is used. The output of FLC controls the switch in the inverter. To control these parameters they are sensed and compared with the reference values. To obtain this the membership functions of fuzzy controller are shown in fig (7).

The set of FC rules are derived from

$$u = -[\alpha E + (1-\alpha)*C] \tag{25}$$

6. SIMULATION RESULTS

The dc component extraction method is implemented and tested in MATLAB/Simulink by using fuzzy logic controller. Simulation results of the dc component extraction method under frequency deviation and with harmonics are shown in Fig. 12. Fig. 12(a) shows the measured ac side current signal which contains

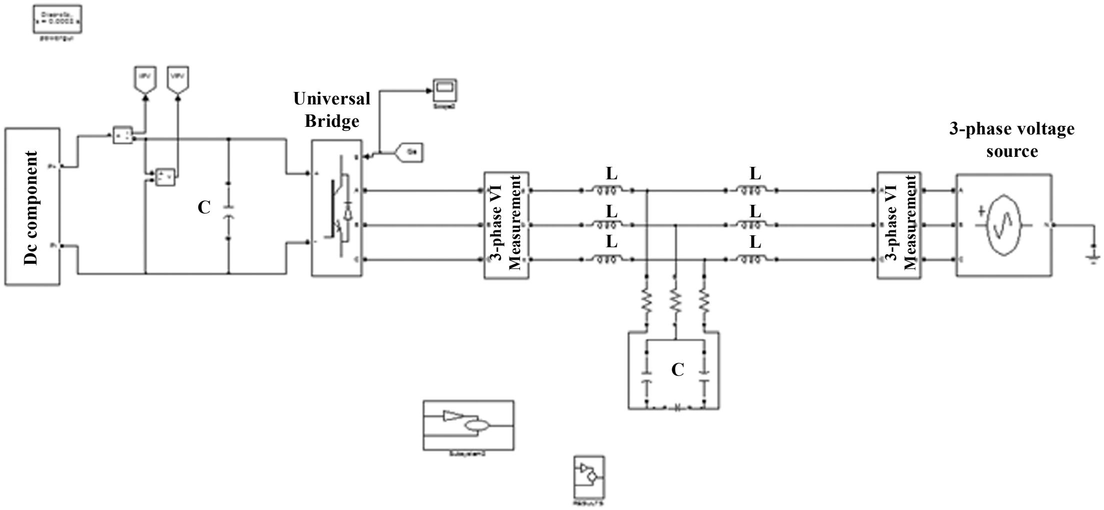

Figure 10: Simulation System Schematic diagram.

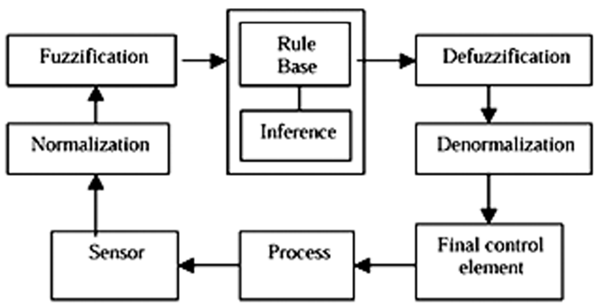

Figure 11: Fuzzy logic Controller

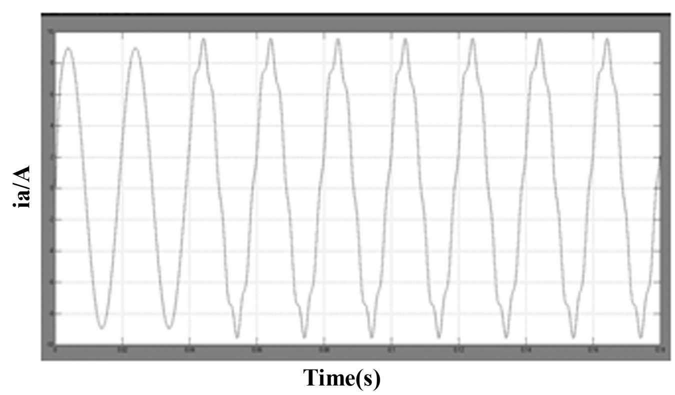

(a) The measured phase A current i_a

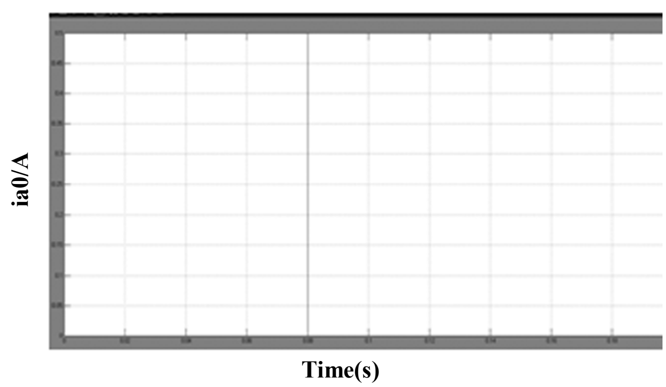

(b) The superposed dc component

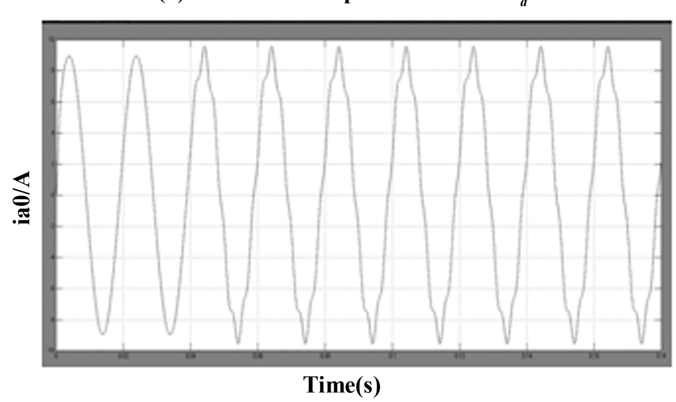

(c) The dc component extraction result with one time integral

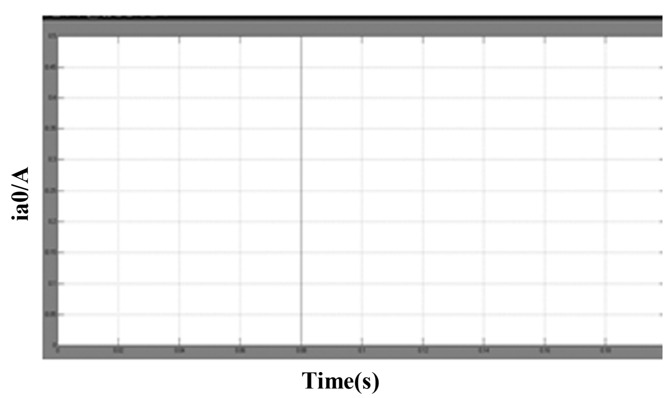

(d) The dc component extraction result with two time integrals.

Figure 12: Simulation results of the dc component extraction method with harmonics and frequency deviation.

fifth and seventh harmonics as well as a dc component appearing from 0.08s. Fig.12 (b) shows the dc component in the current signal with amplitude of 0.5A. Fig. 12(c) shows the simulation results of the dc component extraction method. As seen, althoughthe average value of the dc component is estimated correctly as 0.5A, line frequency fluctuation exists in ia0because of the frequency deviation. However, compared to the original current $i_a$in Fig. 12(a), the ac components have been attenuated effectively. To further eliminate the ripple on the extracted dc component in Fig. 12(c), a second time integral is added over the result obtained in Fig. 12(c), with which the ripple can be effectively attenuated, and the result is shown in Fig. 12(d). As seen, the exact dc component can accurately reflect the original dc signal after a short transition time. Note that the measuring time of one time integral is one line frequency period T_1, and double time integral requires $2T_1$. With more integral times, the precision of the measurement is higher but the measuring time is longer. In practice, two time integrals can achieve both satisfactory precision and measuring speed. In addition, offset in sensors, signal conditioning circuits, and A/D chips have negative impact on the component measurement as well. These biases should be calibrated either online or offline and need to be subtracted from the measuring results. In this way, the influence of the biases can be eliminated.

7. CONCLUSION

This paper has presented an effective method to reduce the dc component in a three-phase transformerless grid-connected PV system. The dc component can introduce line-frequency power ripple in the system and further cause dc-link voltage ripple and second-order harmonics in the ac currents. A software-based “virtual capacitor” approach has been implemented to minimize the dc component via a feed-forward of the dc component.Here fuzzy controller is used compared to alternative controllers because of its accurate performance.The Simpered Systems tool has demonstrated that the joint system will at the same time inject maximum power from a PV unit and compensate the harmonic current drained by nonlinear loads.The dc component can be accurately obtained using the descending window iteration and double time integral even under frequency variation and harmonic conditions. A PIR controller has been planned to allow the precise regulation of both the dc and line frequency components in the *d-q* frame

The proposed method can be well adopted in the existing PV systems for dc component minimization by adding software programs for dc-component extraction, dc-component feed-forward term as well as the resonant controller in the current control loops.

REFERENCES

[1] R. Gonzalez, E. Gubia, J. Lopez, and L. Marroyo, “Transformer less single-phase multilevel-based photovoltaic inverter,” IEEE Trans. Ind. Electron., vol. 55, no. 7, pp. 2694–2702, Jul. 2008.

[2] S. B. Kjaer, J. K. Pedersen, and F. Blaabjerg, “A review of single-phase grid-connected inverters for photovoltaic modules,” IEEE Trans.Ind. Appl., vol. 41, no. 5, pp. 1292–1306, Sep./Oct. 2005.

[3] E. Koutroulis and F. Blaabjerg, “Design optimization of transformerless grid-connected PV inverters including reliability,” IEEE Trans. PowerElectron., vol. 28, no. 1, pp. 325–335, Jan. 2013.

[4] B. Gu, J. Dominic, J. Lai, C. Chen, T. LaBella, and B. Chen, “High reliability and efficiency single-phase transformerless inverter for grid-connected photovoltaic systems,” IEEE Trans. Power Electron., vol. 28, no. 5, pp. 2235–2245, May 2013.

[5] S. V. Araujo, P. Zacharias, and R. Mallwitz, “Highly efficient single-phase transformerless inverters for grid-connected photovoltaic systems,” IEEE Trans. Ind. Electron, vol. 57, no. 9, pp. 3188–3128, Sep. 2010.

[6] O. Lopez, F. D. Freijedo, A. G. Yepes, P. Fernandez-Comesaa, J. Malvar, R. Teodorescu, and J. Doval-Gandoy, “Eliminating ground current in a transformerless photovoltaic application,” IEEE Trans. Energy Convers., vol. 25, no. 1, pp. 140–147, Mar. 2010.

[7] A. Ahfock and A. J. Hewitt, “DC magnetisation of transformers,” IEEProc. Electro Power Appl., vol.153, no.4, pp. 601–607, Jul. 2006.

[8] B. Wang, X. Guo, H. Wu, Q. Mei, and W. Wu, “Real-time DC injection measurement technique for transformerless PV systems,” in Proc. IEEE2nd Int. Power Electron. Distribution Generation Syst., Hefei, China, Jun. 2010, pp. 980–983.

[9] W. Li, L. Liu, T. Zheng, G. Huang, and S. Hui, “Research on effects of transformer DC Bias on negative sequence protection,” in Proc. Int.Conf. Adv. Power Syst. Automat. Protection, Beijing, China, Oct. 2011, pp. 1458–1463.